621.385.833

ELECTRON MICROSCOPY OF MAGNETIC STRUCTURES OF BULKY OBJECTS

V. I. PETROV, G. V. SPIVAK, and O. P. PAVLYUCHENKO

Moscow State University

Usp. Fiz. Nauk 102, 529—548 (December, 1970)

ELECTRON-optics methods have by now found wide application in the investigation of various magnetic structures. Contributing to this were the sufficiently high resolution, good contrast, high sensitivity to the deflecting action of magnetic fields, and the practical absence of electron inertia, making it possible to observe the dynamics of fast processes.

The present article is a review of electron-optical methods of observation, and of qualitative and quantitative estimates of magnetic structures on the surface of bulky objects.

The results obtained with the aid of other methods can be found in[1-4].

I. THE REPLICA METHOD

Low resolution, inertia, and coagulation of the heavy particles are the shortcomings of the Bitter-Akulov powder method, which is widely used to observe the main structures on surfaces of ferromagnets. The resolution of such a method was increased by diluting the powder concentration and by observing precipitation figures obtained from the investigated surface (replica with extraction) in a transmission electron microscope[5,6]. The pictures obtained in this manner for the domain structure on the hexagonal plane of magnetoplumbite[7] or Co[8] revealed many new subtle details (Fig. 1). Such powders were used to investigate the magnetic structure of high-coercitivity CoP films with an easy-magnetization axis perpendicular to the plane of the film[9], and the magnetic structure on surfaces of permanent magnets[10]. The powders were also replaced by ferromagnetic-material vapor precipitated on the investigated surface[11]. No definite connection was found between the magnetic field on the surface and the powdered-precipitate density distribution which determines the image contrast in the electron microscope[12]. An estimate of the resolving power has shown that it is impossible to observe magnetic-field differences in sections smaller than 2000 Å.

Unique "prints" of the magnetic field on a surface are obtained by the "modulation-film" method[13,14]. It turns out that the thickness of polymer films produced on a surface by bombardment with slow (~ 50 eV) electrons is modulated by the local magnetic field. Polymer films on the hexagonal plane of Co, investigated in emission and transmission electron microscopes, duplicate the star-like domain structure. Apparently further increase of the sensitivity and resolution of this method of replicas responding to the microscopic field is promising.

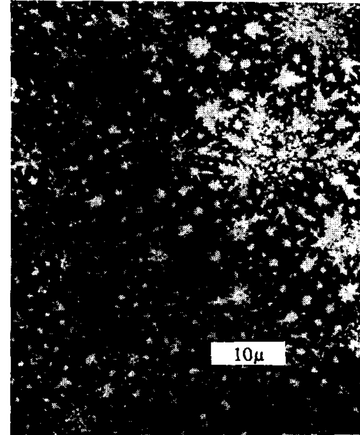

FIG. 1. Electron microphotograph of powder figures on the basal plane of Co [8].

II. THE METHOD OF OBSTRUCTIONS AND SHADOWS. ELECTRON DIFFRACTION IN TRANSMISSION AND REFLECTION

Electron beams were first used to observe magnetic microscopic fields from domain structures in[15]. Electrons with 30 keV energy were scattered from the hexagonal plane of a demagnetized Co single crystal, and a complicated picture of intertwining arcs was obtained on a photographic plate. An estimate was shown that at the surface itself the magnetic fields reach 10^4 Oe, and the field extends to ~ 10 μ above the surface. When the sample was heated, the picture changed[16]. The procedure only revealed the presence of a magnetic field, but did not make it possible to determine its configuration.

A more perfect method was that of "obstructions"[17,18], which is the analog of the Toepler method in electron optics. A transparent disk is placed in the focus of an electron lens, in the image space, and absorbs all the rays if there are no perturbing fields in the object space. If magnetic or electric fields are present in the latter space, the ray paths are disturbed, and the deflected electrons pass to a screen and produce an image. The method was verified with Ni-Co wire of 0.12 mm diameter, magnetized by pulses of alternating polarity, and the image represented periodic light sections against a dark background. The same method was used to observe the stray fields at the boundaries of crystal grains in a magnetized sample in the form of a blade[18].

Subsequently,[19] this method was improved and the field image was obtained by distorting the picture of a grid placed in the image space. From the distortion of

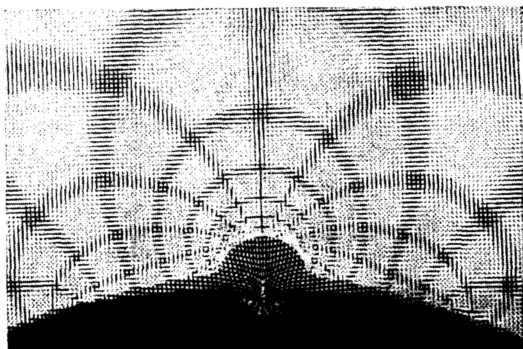

FIG. 2. Moire pattern obtained by aligning the electron-optical shadow images of grids, distorted by magnetic fields of opposite signs from the recording head of the tape recorded Yauza-5 (current ± 1 mA). Below—geometrical shadow of the head, above—moire pattern. On the shadow of the head is the image of the grid distorted by a field having a large gradient in the immediate vicinity of the gap. The lines joining the horizontal and vertical segments observed on the moire pattern characterize the geometric locus of the points for which the tangential and normal components of the field, respectively, are constant [27].

the image it was possible to determine the angular deflections of the electrons and the field distribution. This method was used to observe domains on the edge of a Co crystal[20] and to measure the field at the corner of a Co crystal. The field was 3000 Oe near the surface and 100 Oe at a distance 0.4 mm from it[21]. The same method was used to measure the stray fields of a number of other ferromagnets. Temperature-induced magnetic transformations were also observed: the distortions of the grid image almost vanished when a Co crystal was heated to 670°K[23,24]. A review of this method was published in[25]. The grid method was recently used[26,27] to investigate the stray fields of magnetic-recorder heads and of different magnetic materials. The distortion produced by the magnetic field was superimposed on the undistorted image of the grid. This led to the formation of a moire pattern, the geometrical picture of which in many cases is a topographic map of the components of the investigated magnetic field (Fig. 2). We note that the resolution of the "grid method" is limited in principle by the size of the mesh of the grid.

The method of investigating magnetic fields by means of the distortion of the shadow of an extraneous body was used for a qualitative and quantitative investigation of the stray fields of 71°-domain Bloch boundaries in Ni single crystals[28-35]. A thin ribbon beam shaped by special knife-edge diaphragms glanced along the domain boundaries. The value of the field at different distances from the sample was investigated by displacing the beam. The results of the investigation have shown that the structure of the stray fields at the edge of a single crystal depends strongly on the angle between the (110) plane and the investigated face. With increasing angle between them, owing to the decrease of the density of the magnetic charges on the surface, the normal component of the field increases. The most interesting results were obtained by investigating the stray fields of elongated Bloch boundaries of cylindrical Ni crystals[35]. It was found that the boundary has a dipole charge—the poles are located on both sides of the boundary in a region of 10—15 μ in the direction of the crystal axis, while the boundary itself has no charge. The maxima of the magnetic-field component normal to the surface of the crystal are equal to ~ 25 Oe and are located at a distance 4—10 μ. A special microscope was later developed[36] to carry out such investigations. A somewhat modified method was used to investigate needles of Fe, Ni, and Ni-Co of 0.5—5 μ diameter in a transmission electron microscope operating in the focused mode[37-38].

When the aperture diaphragm is located off-center, the shadow of the diaphragm on the image is displaced as a result of the action of the magnetic stray fields near the sample on the electrons. The sample magnetization determined from this displacement was in satisfactory agreement with the value known for iron[37]. A comparison of the measurement data with those calculated by means of simple models has led to certain conclusions concerning the distribution of the magnetization in such crystals.

Another simpler and clearer method is the shadow method (where the shadow of the object itself is investigated)[29]. It does not give detailed quantitative information, but the ease with which the image can be interpreted and the simplicity of the apparatus have contributed to its extensive utilization in the investigation of the domain structure and of magnetic transformations. The observations were first carried out with an electronograph and very small diaphragms were used (~ 6—10 μ) to obtain a thin electron beam to produce the shadow image (Fig. 3), but the brightness of the image was very low. This inconvenience was subsequently eliminated by using a scanning system, which moved the electron probe along the edge of the object, making it possible to observe the picture on the screen[40-42]. The theory of image formation was verified with an artificial sample—a model of a multidomain crystal[43]. This method was used to investigate crystals of Co[39,41,44], hematite[40,45-48], magnetite[40,49], barium ferrite[42], and gadolinium and ytterbium iron ferrites[50], and also magnetic fields connected with the superconducting state of matter[51-53]. The measured domain width was 40—240 μ for Co, ~ 250 μ for hematite, and 60 and 30 μ for natural and artificial magnetite, respectively. Temperature investigations have shown the following: 1) an appreciable decrease of the stray fields for Co with increasing temperature and their complete vanishing at 520—560°K (the crystal became isotropic and closing domains were produced); 2) almost complete vanishing of the stray fields for hematite at temperatures below 260°K, where its magnetic transformation takes place;

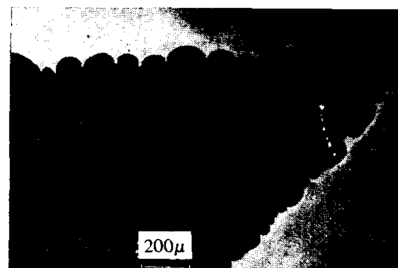

FIG. 3. Shadow image of the edge of a single crystal of Co, obtained by using a point source of electrons [39].

a memory effect was observed—the picture of the stray fields was completely restored when the temperature was changed in the opposite direction; measurement of the Curie point yielded 916—965°K for different hematite samples; 3) for magnetite, the appearance of stray fields was observed when the temperature was lowered to 120°K, and the memory effect was usually not observed; 4) for the iron garnets, partial and complete vanishing of the stray fields was observed.

The theory of image formation in the shadow method is not complicated and can be found in the fairly complete review[54]. The main shortcoming of all shadow methods is that they make it possible to observe only one-dimensional structures and are not suitable for the investigation of complicated domain structures on surfaces of bodies.

The method of electron diffraction in reflection and in transmission has been used for a magnetic analysis of bulky objects and thin films[55,56]. The Lorentz shift of the reflections and of the circles makes it possible to determine the direction of the magnetization and to estimate its magnitude. Thus, for magnetite, it was found[57] that the easy-magnetization axis is [111] and that the saturation induction is ~ 9600 G. Temperature investigations with an electronograph[58] have shown that the magnetite compensation point is ~ 300°K. It was found that the easy axis of Fe single crystals[59] coincides with the [100] axis, and the saturation induction is 20,000 G. Similar investigations were made for single crystals of Co[60], single crystals and films of Ni[61], invar[62], films of Ni and Fe[63], NiFe[64], and particles of Fe_3S_4[138]. It was found that the direction of magnetization and of the easy axis of permalloy is [110] and [100], as had been assumed earlier, but in some cases the magnetization direction was [001]. Quantitative estimates of the induction are approximate, since the distance to which the stray fields extend around the sample is unknown.

III. EMISSION MICROSCOPY

In an emission electron microscope[65] the object itself is the source of electrons forming its image. Since the initial velocities of the electrons are relatively low, the system is sensitive to surface microscopic fields. The domain structure can be observed in the secondary or photoemission regimes; thermionic emission is not suitable, since sufficient electron emission occurs at temperatures above the Curie point.

The possibility of producing images of magnetic microscopic fields with the aid of an emission electron microscope was demonstrated by magnetizing[66] a synthetic sample consisting of a stack of Cu and Ni ribbons. An image of the external magnetic fields penetrating into the microscope through a foil window was obtained. The image clarity was poor, owing to the use a relatively simplified glass model of the emission microscope, with an optical system subject to large aberrations. The magnetic contrast, however, was sufficient to draw the first important conclusions, namely, that the focal plane for magnetic surface microscopic fields does not c coincide with the focal plane for the geometric microrelief, and the regions where the magnetic field enters and leaves are represented by dark sections on the

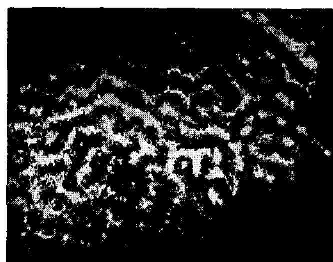

FIG. 4. Image of the main structure on the (0001) plane of a single crystal of Co in an emission microscope with photoelectronic emission [71].

image. A mechanism for forming the magnetic contrast was also proposed, namely, the electrons leaving the surface of the sample wind themselves, as it were, around the magnetic force lines, diverging from the entrance and exit regions and producing noticeable variations of the current density only at a certain distance from the surface.

The same instrument was used to observe for the first time the domain structure on the hexagonal plane of Co[67] and the propagation of temperature waves in a ferromagnet, owing to the contrast between the ferromagnetic phase and the regions that have gone beyond the Curie point[68]. An investigation of the domain structure of heated Co[69,70] has shown that the image contrast decreases with increasing temperature, corresponding to a decrease of the stray fields.

The domain structure of Co was observed in a simplified construction of an emission microscope operating in the photoemission regime[71] (Fig. 4). A photosensitive antimony-cesium layer was produced on the surface of a ferromagnet in a vacuum of 5×10^{-7} Torr, and the emission was produced by illuminating with an incandescent lamp. The image was quite good. One can expect that the resolution and the image quality can be improved by working near the red edge of the photoeffect and by using high grade optics in the microscope.

Many investigations have been devoted to the image formation and to the contrast in an emission microscope. An increase of the accelerating voltage improves the resolution of the immersion object, but simultaneously[72] lowers the sensitivity to the microscopic fields. Thus, a compromise value of the accelerating voltage must be chosen. A certain connection between the magnetic field intensity and the current density on the screen was obtained in[73]. Images with good contrast were obtained in an investigation of the microscopic field of a magnetic recording head[74]. The contrast was due to the interaction between the normal electron velocity v_z and the tangential components H_x and H_y of the magnetic field, namely, the electrons deflected by the tangential field are cut off by the aperture diaphragm, the position of which influences the contrast, and the gap has the form of a dark band on the image (Fig. 5). In another position, the diaphragm can transmit deflected electrons and block the undisturbed ones, and then the contrast becomes negative—the image of the gap field has the form of a light strip against the dark background (the dark-field method).

Further development of the theory of image contrast of magnetic microscopic fields is dealt with in[75-78].

FIG. 5. Image of working surface of a magnetic recorder head in an emission microscope with an aperture diaphragm, with the magnetizing current flowing through the winding of the head [76]. The figure shows the gap region in the form of a dark band.

The direct and inverse problems were solved in first-order perturbation theory under the simplifying assumptions that the magnetic fields are relatively weak and the motion of the electrons along the optical axis z is determined only by the accelerating electric field E_0. By "direct problem" is meant the determination of the image contrast from the known microfield on the surface of the sample, and by "inverse" is meant the determination of the microfield on the surface of the sample from its image contrast.

The emission microscope can be operated in two regimes: without an aperture diaphragm and with an aperture diaphragm. Since the formation of the contrast differs significantly in these two cases, let us consider each case separately.

1. Operation without aperture diaphragm. The tangential magnetic fields B_x and B_y (the coordinate axes x and y lie in the plane of the sample) lead to a shift of the electron trajectories and to a shift of the points on the image. For homogeneous magnetic fields, there is no image contrast in this regime and the magnetic microfield leads only to a distortion of the image as a result of the unequal displacements of the image points[75]. The expression for the displacement S has the form of a convolution and admits of an inverse transformation[77], i.e., of a determination of B as a function of the sample coordinates x and y from the known function S(x, y):

$$B_{0y}(x, y) = -\frac{9\sqrt{E_0 m}}{2\sqrt{2\pi e}\left[\Gamma\left(\frac{1}{4}\right)\right]^2} \times \int_{-\infty}^{+\infty}\int_{-\infty}^{+\infty} \frac{S_x(x-\xi, y-\eta) - S_x(x, y) + \xi\frac{\partial S_x(x, y)}{\partial x} + \eta\frac{\partial S_x(x, y)}{\partial y}}{(\xi^2+\eta^2)^{7/4}}\, d\xi\, d\eta, \tag{1}$$

where e and m are the charge and mass of the electron, E_0 the accelerating electric field, Γ the Gamma function, and B_{0y} the local value of the y component of the magnetic field on the surface of the object (with an analogous definition of B_{0x}). If the field varies only along one coordinate (y), i.e., in the case of homogeneous field, the normal components of the field on the surface is determined from the relation

$$B_{0z}(y) = \frac{1}{\pi}\int_{-\infty}^{+\infty} \frac{B_{0y}(\xi)}{y-\xi}\, d\xi. \tag{2}$$

Expressions (1) and (2) are the solutions of the inverse problem.

To obtain the distribution of the magnetic microfield on the surface of the sample it is necessary in practice to measure the displacements S_x and S_y of the image point, and then perform a computer calculation in accordance with (1). The displacements are determined from the distortion of a regular grid that is sputtered over the investigated surface.

2. Operation with diaphragm. In this regime, the local intensity on the image is determined by electrons passing through a diaphragm, and the image contrast is given by

$$K = j/j_0 = \exp(-S^2), \tag{3}$$

where j is the current density on the image in the presence of magnetic microfields, j_0 is the uniform current density in the absence of microfields, and S is the displacement of the electron trajectories in the plane of the diaphragm as a result of the action of the microfield. The expression for the displacement is in this case a convolution that admits of an inverse transformation, and the solution of the inverse problem leads to the following expression for the field[76]:

$$B_{0y}(x, y) = \frac{\sqrt{V_T}}{\pi\sqrt{2e/m}} \int_{-\infty}^{+\infty}\int_{-\infty}^{+\infty} \frac{S_x(x, y) - S_x(x-\xi, y-\eta) - \xi\frac{\partial S_x(x, y)}{\partial x} - \eta\frac{\partial S_x(x, y)}{\partial y}}{(\xi^2+\eta^2)^{3/2}}\, d\xi\, d\eta, \tag{4}$$

where v_T is the most probable energy with which the electrons leave the cathode (in volts). The function S(x, y) is determined from the contrast on the screen by using (3), and the field is then calculated with a computer from (4). Figure 6 shows plots of B_z and B_x for a magnetic recorder head, with B_z calculated from formula (2). In expressions (1) and (4) it is necessary to substitute the values of the function S in the interval from $-\infty$ to $+\infty$. The experimental values of S, however, are obtained only within a certain finite interval of the coordinates. This makes it necessary to approximate the "tails" of the function S in sections far from the place of localization of the microfield, and naturally introduce a definite error in the calculation of the microfield.

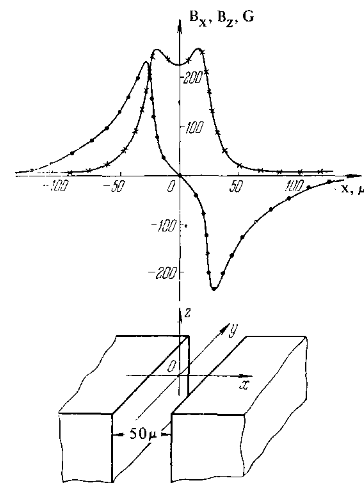

FIG. 6. Distribution of the normal component B_z (points) and tangential component B_x (crosses) of the magnetic field on the surface of a current-energized magnetic-recorder head. The distribution is determined from the contrast of the image in an emission microscope with diaphragm. Below—diagram of gap and coordinate axes.

The use of a number of simplifying assumptions in the calculation also introduces a definite error in the determination of the field. An estimate of some of the errors, including those due to geometric inhomogeneities, can be found in[78-80].

The use of formulas for very localized magnetic fields, for example the stray field from domain boundaries, can lead to a larger error than in the case of fields with larger geometrical dimensions, since even the tangential displacement of the electrons during the time of flight through the region of action of the magnetic microfield cannot be regarded as small as compared with the characteristic dimension of the field.

IV. RASTER MICROSCOPY

In a raster electron microscope, the image is constructed point by point. A system of electron lenses is used to obtain a thin (50—100 Å) electron probe, which is swept over the sample with the aid of a deflecting system. The image is observed on the screen of a cathode ray tube, the beam of which moves in synchronism with the probe. The brightness on the screen of this tube is controlled by the signal from the sample. The resolution of the instrument (50—100 Å) is determined in first approximation by the probe diameter, and the magnification is determined by the ratio of the deflection of the beam in the cathode-ray tube and on the object. A more detailed description of the instrument and its application is given in[81].

It is possible to combine simultaneously in a raster microscope a number of features needed for the observation of magnetic microfields of bulky samples: 1) the observed object need not be planar, 2) the depth of focus is higher by 2—3 orders of magnitude than in the case of the optical or emission electron microscopes; thus, there is no need for polishing and ensuing disturbance of the sample geometry, 3) the signal from a weak magnetic field can be separated from the strong background signal due to the topography by electronic resonant amplification of the video signal or by using slow secondary electrons with a narrow spectrum to construct the image[81,82].

The magnetic microfield recorded on a magnetic tape was observed for the first time in a low-voltage raster instrument by using absorbed electrons[83]; it was subsequently observed in an ordinary raster microscope[84-94]. The contrast of the magnetic recording is manifest in the form of light and dark bands. Besides the structure of a magnetic recording, the domain structure on the surface of the Co was also made visible (Fig. 7)[85,86], and the sensitivity to the magnetic microfields was increased by proper choice of the potentials on the collector system, which served as a velocity analyzer, and the image was produced only by secondary electrons with narrow energy spectrum. The image of the magnetic structure was superimposed on the picture of the microgeometry of the surface, but the latter could be eliminated by a compensation method, using a signal of opposite phase from another collector. The detector could be tuned to the vertical or horizontal component of the magnetic field[86]. The diaphragm diameter was chosen to effect a compromise between sensitivity and signal loss[87]. A "Stereoscan" microscope was used

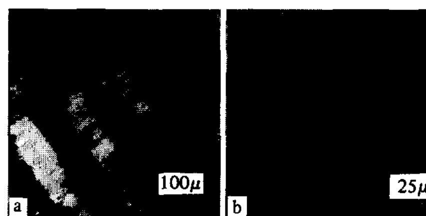

FIG. 7. Image of an inscribed magnetic tape (a) and of the domain structure on the surface of a Co crystal (b), obtained with a raster electron microscope [85,86].

to investigate the dependence of the contrast of the domain structure of cobalt on the voltage between the collector and the sample[88]. It was observed that the magnetic contrast is very sensitive to this voltage, and also to the orientation of the sample relative to the collector. The accelerating voltage of the probe was 4.5—5 kV, and the resolution was ~ 1 μ. The domain structure of ferrite and the temperature variations of the domain structure of Co were also observed[89]. The contrast decreased sharply with increasing temperature and disappeared at 240°C (a temperature at which the anisotropy constant K_1 became negative). It is assumed that the magnetic contrast from the domain structure is determined not by the stray fields of the domain boundaries themselves, but by the magnetic charges produced on the domain surfaces because the sample plane is not parallel to the hexagonal axis.

For the usual arrangement of the electrodes and for the usual potentials on them, the direct problem of theoretically determining the contrast in a raster microscope has been solved only qualitatively[90,91]. This is due to the fact that the microfield at the object in a raster microscope is of the same order as the field accelerating the secondary electrons. It is therefore impossible to linearize the equations (there is no small parameter). In addition, it is difficult to take into account the geometry of the electrodes exactly. Application of a strong accelerating field[92,93] makes it possible to linearize the equations of motion, but the sensitivity of the microscope to the microfield is thereby reduced[72]. A qualitative analysis of the contrast has made it possible to show that its value is quite sensitive to the collector voltage, to the position of the slit, and to the maximum value of the magnetic field in the magnetic-recorder-head gap. Depending on the values of these quantities, the image of the gap can have the form of either a light or a dark band[90,91]. This microfield was observed experimentally in an instrument with increased sensitivity[94] by resonant amplification of the collector signal, modulated either by the alternating field of the head or by the alternating intensity of the electron probe illuminating the object (Fig. 8). Measurement of one-dimensional magnetic fields can also be carried out by using a modified grid method[18], with the distribution and magnitude of the fields determined from the distortion of the image of the grid[95-97]. Moire patterns were obtained in this manner in[97]. The use of the cathode-luminescence regime excludes the influence of the secondary electrons[139]. The magnetic fields can also be estimated from the distortion of the pseudo-Kikuchi lines[140].

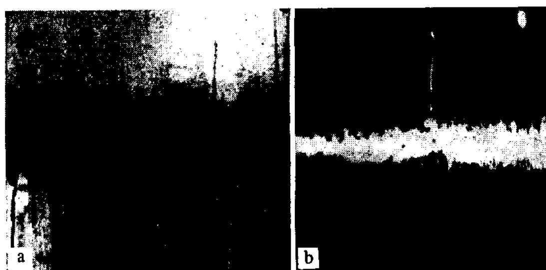

FIG. 8. Image of the magnetic field in the gap of a magnetic recorder head, obtained with a raster microscope in the resonant amplification regime [94]: a–bright field image b–dark field image.

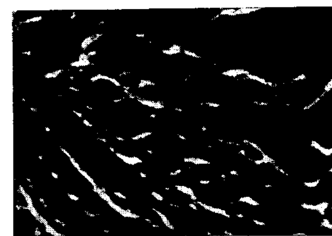

FIG. 9. Image of the domain structure on the hexagonal plane of single-crystal Co, obtained with an EMM [106].

V. MIRROR MICROSCOPY

The basic unit of the electronic mirror microscope (EMM) is the electronic mirror—an immersion mirror objective (consisting in the simplest case of a flat sample, a cathode with a diaphragm, and an anode). The lens system forms the probing beam and transfers the image to a screen. The beam electrons are decelerated in the field of the mirror objective, are returned from the surface of the object, and are accelerated by the same objective field which had previously decelerated them, producing the image of the surface of the sample on the instrument screen. The essential features are the following: 1) the electrons do not bombard the sample, 2) the low velocity of the electrons as they move in both directions at the surface of the object makes for a high sensitivity to the perturbing microfields and leads to a high image contrast.

In addition to a simple two-electrode objective, one uses also more complicated three- and five-electrode electrostatic[98] and magnetic[99] objectives. Data on EMM designs can be found in[100-103].

The EMM can operate in two regimes: the scattering or shadow regime, and the focused regime. In the latter, where the contrast is determined by the aperture diaphragm, the attained brightness is larger and the resolution better[104], and the reproduction of the object is also more faithful[105].

For investigations with the EMM, the sample surface must be carefully polished, otherwise the contrast from the microrelief distorts the image of the microfields. Ferromagnetic objects should furthermore be annealed and subjected additionally to weak electric polishing.

The possibility of observing magnetic microfields in an EMM was first demonstrated in[106] using a special sectionalized sample consisting of alternating magnetic and nonmagnetic strips, magnetized normal to the surface. The contrast was the inverse of the contrast in the emission microscope—the light sections corresponded to the presence of the field H_z. The image of the domain structure on the hexagonal plane of a single crystal of Co was also observed (Fig. 9). The image contrast was very strong. A comparison[13,107] has shown that the powder-figure image agrees with the electron-mirror image.

The formation of magnetic contrast in the EMM was analyzed qualitatively in[108]. Experiments were performed on a composite magnetized sample and on a magnetic-recorder head; grids were sputtered over the surface of the samples. It was observed that the magnetic microfield causes deformation of the grid image, and the following criteria were deduced for distinguishing between the image of the magnetic structure and the image of the electric and geometric relief:

1) The magnetic contrast is the result of the action of the normal component of the magnetic field on the radial component of the electron velocity, and therefore the sensitivity of the EMM to magnetic fields vanishes in the optical center of the sample, where the radial velocity of the electrons is equal to zero, and increases towards the periphery.

2) The regions in which $\Delta B_z/\Delta\varphi > 0$ produce bright images and those with $\Delta B_z/\Delta\varphi < 0$ are dark, the contrast is inverted so that when a region moves through the optical center (φ is the azimuth angle).

3) Radial magnetic structures have a larger contrast than azimuthal ones.

4) The round secondary-emissions spot in the center of the image is deformed in the presence of tangential components of the magnetic microfields (this sometimes takes place also under the influence of electric microfields).

The foregoing criteria were corroborated by a simplified quantitative analysis of the electron motion.

The same paper describes also a study of the domain structure on single-crystal Ba and Ni ferrites.

Further improvement of the electron-optical characteristics of the mirror system has made it possible to increase its sensitivity and the quality of the images of the magnetic structures[13,109]. Weaker stray fields were observed on multiaxial crystals of iron and silicon iron with closed magnetic flux lines. The domain structure was observed on the hexagonal plane of a Co sample magnetized normally to the investigated surface. Also observed were the magnetic structure of silicon iron following application of a magnetic field normal to the surface[110,111], the magnetic stray fields on the grain boundaries of silicon iron following magnetization[112], and the strip domains in films of 90% Ni–10% Fe of 1 μ thickness[113]. A comparison of the powder figures and of the EMM image showed good agreement[114].

A regular structure of antiparallel domains was observed on the prismatic plane of single-crystal Co[115]. The system of parallel domains was displayed in the form of wedges (Fig. 10). The direct images of the boundaries were the bright edges of the wedges. The image of the boundary was rotated relative to the boundary itself, and was brighter as a result of the narrowing of the picture of the place where the field was localized[116,117]. A more detailed analysis has shown that the bright edges are caustics due to the action of the periodic structure[135].

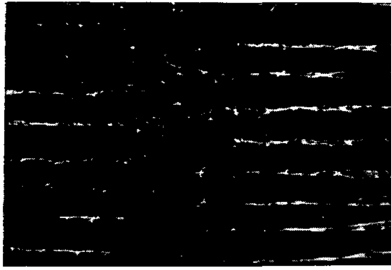

FIG. 10. EMM image of the domain structure on the prismatic plane of a Co single crystal [115].

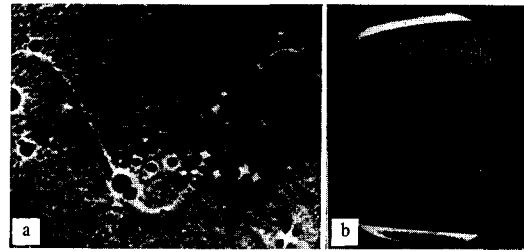

FIG. 12. EMM image of magnetic recording: a) on a film [119] b) on a magnetic-recorder tape [120].

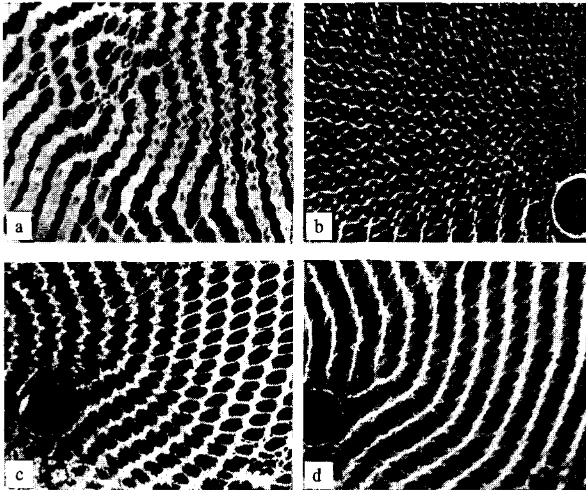

FIG. 11. EMM image of a complicated domain structure in the (0001) plane of magnetoplumbite at different orientations of the domain structure relative to the optical center and at different heights of the electron reflection over the surface. Optical center–top (a), right (b), bottom (c), right (d) (the radial structures on the image have a larger contrast than the azimuthal ones), Bias voltage: c–1V, d–5V (the dimension of the stray fields of different sections of the domain structure are different) [118].

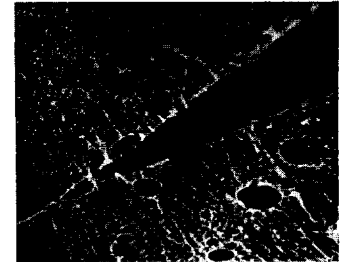

FIG. 13. EMM image of the magnetic field in the gap of a current-energized magnetic-recorder head (dark wedge) [74].

In spite of the difficulties involved in interpreting even linear one-dimensional structures, two-dimensional domain structures sometimes give very clear pictures, for example the domain structure on the (0001) plane of single crystals of Co and magnetoplumbite[118]. In this case the distortions due to the geometric relief are greatly reduced by very careful preparation of the surface, which has made it possible to obtain photographs of high quality (Fig. 11).

The inhomogeneity of the field along the domain is revealed when the orientation of a section of the sample is rotated 90° relative to the optical center (Fig. 11 a and b). In this case the strong picture of the domain itself gives no contrast, but its periodic variations in the longitudinal direction, owing to the star-like regions of inverse magnetization, produce a picture in reticular form. The contrast is not very high, owing to the lower intensity and smaller dimensions of the fields of the "stars." When the domain orientation relative to the radial direction is $\sim 45°$, both the strong domain boundaries and the weaker boundaries of the "stars" are processed: the image is similar to a honeycomb with hexagonal cells (Fig. 11 c). A slight change of the orientation and moving away of the reflection surface from the object ($U_b = -5$ V) greatly reduce the contrast of the "star" boundaries, although the domain boundaries remain sufficiently bright (Fig. 11d). Their contrast can be decreased by the same amount only with a negative bias of -50 V, i.e., when the electrons are reflected at a height $\sim 25\ \mu$.

Consequently, the effective dimension of the stray fields of the small area with inverse magnetization inside the domain are smaller by one order of magnitude than the dimensions of the field of the main domain, and amounts to 2–3 μ.

An interesting application of the EMM as a reading device for magnetic recording was proposed in[119]. Figure 12a shows the image of magnetic recording on a MnBi film saturated perpendicular to the surface. The recording was made by local heating above the Curie point, using a hot pen. A similar recording can be made by heating with an electron probe, and read subsequently in the mirror regime. The recorded line is a section magnetized in a direction opposite to that of the remaining surface. Magnetic recording on a recorder tape was made visible in[120,74] (Fig. 12b). It was observed[121] that the sensitivity with which magnetic-tape recording can be visualized is increased if the sample is inclined to the optical axis of the mirror objective, owing to the increase of the tangential velocity of the electrons along the magnetic trace. The authors propose that the tape can be placed outside the vacuum and read through a mica window, and that such a system can produce a resolution ten times better than ordinary reproducing magnetic heads. The sinusoidal field of the recording was measured in[122,123].

One of the magnetic objects investigated in greatest detail in EMM is the magnetic-recorder head[108,74]. The field of the head has relatively large dimensions, and its magnitude can be readily adjusted. The gap region in the presence of a magnetic field (Fig. 13) produces a picture in the form of a dark wedge[74], the orientation of which depends on the field direction. This "wedging" of the image can be seen also on the photographs of[108], where no significance was attached to it,

it being noted only that the field of the gap produces a certain distortion of the grid image. The mechanism governing the contrast of the image of the field of a magnetic-recorder head was already considered qualitatively in[74]. With increasing current (H_Z increases), the aperture angle of the wedge increases and the dark region broadens. The increase of the angle with increasing H_Z is due to the growth of the azimuthal displacement of the electron trajectories on the edges of the gap. The obtained coefficient of the linear dependence of the wedge angle on the magnetizing current is valid only for a magnetic field of a given configuration.

The decrease of H_Z with increasing distance between the working surface and the gap is first very rapid, and then slows down. Even at a distance 20 times the gap width, H_Z still produces a noticeable shift of the surface image.

The EMM makes it possible to observe not only static fields of the head, but also the dynamic fields when the stroboscopic regime is used[124]. The stroboscopic regime is realized by applying unblocking strobe pulses, in synchronism with the alternating current feeding the winding of the magnetic-recorder head, to the modulator of the normally cut-off electron gun. The screen shows a static image formed at the same instant of time of each period of the alternating process. By varying the delay between the strobe pulses and the current in the head, it is possible to observe different phases of the process. Such a regime makes it possible to investigate the frequency properties of magnetic-recorder heads. The frequency characteristic of the head is obtained by selecting an equivalent direct current for each frequency. It turned out that for most heads the form of the field distribution remains unchanged with changing frequency, so that it is possible to choose an equivalent direct current that produces the same field over the gap as the alternating current. The phase characteristic is defined as the phase shift between the maximum field (maximum wedge angle) and the maximum current.

This method is very convenient in that it makes it possible to monitor directly the magnetic field of the heads, and is successfully used to investigate dynamic characteristics of heads[122,123]. Weak magnetic fields can be observed by using the resonant amplification method. Thus, in[125] this method was used to obtain the image of the field of a magnetic-recorder head at a magnetizing current of only $\sim 6\ \mu A$ (there was no contrast in the usual regime). Certain applications of EMM for the investigation of magnetic structures are given also in[126].

Since the formation of the magnetic contrast in the EMM and its interpretation are complicated processes, let us consider in greater detail the theory of contrast formation in the EMM. The first quantitative estimate of the magnetic contrast[127] has led to a linear dependence of the contrast on the first derivative of the normal component of the magnetic microfield. In that reference, just as in[115], no attention was paid to the scale distortion: in an EMM working in the shadow regime, as in any shadow instrument, there is always scale distortion on the screen, i.e., the coordinates of an image point on the screen are determined not only by the magnification of the system and by the position of the sample point producing the image, but also by the local value of the microfield. Thus, when an attempt is made to construct the distribution function of the contrast[127] as a function of the coordinates of the screen, the question arises as to which coordinates of the screen must be set in correspondence with the coordinates of the samples.

In addition, as shown by further investigations, the contrast is not determined in general by the first derivative of the field[116,128]. In this connection, the results of[114,129,130], where this approximate expression was used for the contrast, do not give sufficiently rigorous results concerning the magnetic field. The use of an "effective" dimension z_0[114] is justified if a criterion for the determination of z_0 were to be given (as was done in[116]). The value of z_0 depends on the field configuration, and can be determined only if one knows the field distribution. In addition, the resolution of the instrument in these experiments[129,130] was possibly insufficient to obtain data on the internal structure of the boundary. For a one-dimensional magnetic field with a known distribution it is possible, by using simple relations, to determine its maximum value from the angle of rotation of the image. The fields of an artificial sample—a ferromagnetic strip—were measured in this manner at different values of the magnetization in the direction normal to the surface[116]. The results were in good agreement with the results of measurements by the ballistic method. The rotation of the image was used also to estimate the field of superconducting sections of a niobium sample in the intermediate state[131].

A more rigorous approach to the problem of magnetic contrast for weak microfields was developed in[128,132,117,133,134]. The same simplifications were used as for the emission microscope. For the case of small perturbations, the azimuthal displacement of the electron trajectories on the screen, under the influence of the magnetic microfields, is given by

$$S(X) = \gamma(X) R, \tag{5}$$

where $\gamma(X)$ is the local angle of rotation on the image, and R is the distance from the point on the screen to the optical axis. The contrast is connected with the displacement of the electron trajectories as a result of the action of the microfields:

$$j(X') = j/[1 + (dS(X)/dX)], \tag{6}$$

where $j(X')$ is the current density on the screen at the point $X' = X + S(X)$, and X is the coordinate of the place where the undeflected electron strikes the screen. The expression for γ has the form of a convolution, and the solution of the inverse problem leads to the following expression for the normal component of the magnetic field on the surface of the sample:

$$B_{0z}(x, y) = A\sqrt{\frac{E_0 m}{e}} \int_{-\infty}^{+\infty}\int_{-\infty}^{+\infty} \frac{\gamma(x, y) - \gamma(x-\xi, y-\eta)}{(\xi^2+\eta^2)^{5/4}}\, d\xi\, d\eta, \tag{7}$$

where A is a coefficient that depends on the geometry of the objective.

Thus, to determine the microfield it is necessary to know the local angle of rotation of each point of the image. This can be done directly by measuring the angle or the displacement on the photograph of the image. To this end, a film of nonmagnetic material is sputtered on the sample through a regular grid with sufficiently fine

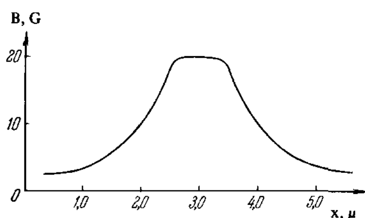

FIG. 14. Distribution of normal component of the magnetic field on the surface of a magnetized ferromagnetic strip, as determined from the displacements of the points on the image of the strip in the EMM with the magnetizing current turned on and off [117].

FIG. 15. Determination of the displacements from the integral curves (integral of the current on the image). I_0—no perturbing field, I_1—in the presence of a perturbing field [117].

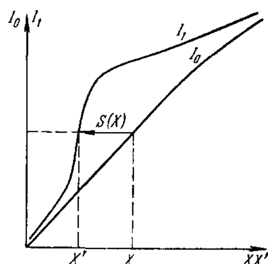

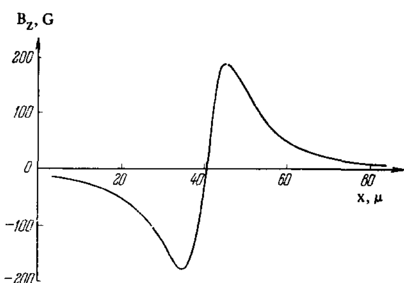

FIG. 16. Distribution of the normal component of the magnetic field on the surface of a magnetic-recorder head when magnetizing current flows; the distribution is determined from the displacements obtained from the integral curves in the EMM [117].

mesh. The displacements are determined from the distortion of the image of the grid. A computer is then used to calculate the field from the displacements by means of formula (7). This was done[117] for a sample with a ferromagnetic strip (Fig. 14). In addition, for one-dimensional fields that can be turned off, the displacement can be determined from the integral curves (the integral of the electron current on the image) (Fig. 15).

This method was used to obtain[117] the dependence of the normal component of the magnetic field of a magnetic-recorder head (Fig. 16). For a one-dimensional field, formula (2) can be used to calculate also the tangential component. The measurement of the displacements by means of a photograph is a more sensitive method than the integral-curve method. The displacements on the image are already appreciable before the contrast becomes noticeable.

If it is known beforehand that the field varies like $B_{0Z}(x) = B_0 \cos \omega x$, the expression for the contrast takes the form[122,123]

$$K(X') = [1 - A_1 \omega^{1/2} \exp(-\omega h) B_0 \sin \omega x]^{-1},$$
$$X' = X + M A_1 \omega^{-1/2} \exp(-\omega h) B_0 \cos \omega x, \quad (8)$$

where $A_1 = (R/M)\sqrt{\pi e l/2mV_0}$, M is the magnification of the EMM, h is the height of the reflection of the electrons, and l is the distance from the sample to the diaphragm. To determine the displacements, the integration can be carried out from a point where the displacement is equal to zero—the density current is minimal or maximal. In this case it is not necessary to demagnetize the film or to sputter on it a scale grid. However, this procedure cannot be used even for arbitrary periodic fields.

A check on the measurement accuracy for a sample with a known field distribution—a current-carrying wire[133,134]—has shown that the method has sufficient accuracy, 10–15%. However, all the remarks concerning calculations with an emission system remain in force also in this case. The reduction of the EMM system to a shadow-projection system[135] has made it possible to estimate the influence of the finite dimensions of the electron source on the image contrast and to write down relations for the diffraction contrast of magnetic structures in the EMM.

In conclusion we note an interesting use of a hybrid instrument—a raster electronic mirror[136,137]—for the investigation of magnetic microfields. In this instrument the high sensitivity of the EMM to the microfield is retained, but there are no image distortions (wedging, etc.). It should be borne in mind here that the raster microscope has its own peculiarities, since the resolution depends on the diameter of the probing beam, whose dimensions can be increased in the decelerating fields.

The resolution of the emission, mirror, or raster devices (~ 100 Å) is inferior to that of the 100 kV transmission electron microscope (several Å). At the same time, these three instruments make it possible to study qualitatively and quantitatively the properties of magnetic structures of bulky objects, something that cannot be done even by an high-voltage transmission electron microscope with $(1.5-3.0) \times 10^6$ V, the use of which is so far limited to micron thicknesses.

The intensive development of microscopy gives grounds for expecting for further progress in the study of magnetic structures with even better image quality.

At the same time, great progress has already been attained in the use of transmission electron microscope for the investigation of magnetic structures of thin films.

[1] R. Carey and E. D. Isaac, Magnetic Domains and Techniques for their Observation, Academic Press, New York, London (1966).

[2] D. J. Craig, J. Appl. Phys. 38, 931 (1967).

[3] S. V. Vonsovskiĭ and Ya. S. Shur, Ferromagnetizm (Ferromagnetism), Van Nostrand, 1945.

[4] Translation collections: Magnitnye struktury ferromagnetikov (Magnetic Structures of Ferromagnets), ed. by S. V. Vonsovskiĭ, IL, 1959; "Magnitnye svoĭstva metallov i splavov" (Magnetic Properties of Metals and Alloys), ed. by S. V. Vonsovskiĭ, IL, 1961; S. V. Vonsovskiĭ, Usp. Fiz. Nauk 90, 491 (1966) [Sov. Phys.-Usp. 9, 874 (1967)].

[5] D. J. Craik, Proc. Phys. Soc. B69, 647 (1956).

[6] D. J. Craik and P. M. Griffiths, Brit. J. Appl. Phys. 9, 279 (1958).

[7] L. F. Bates, D. J. Craik, P. M. Griffiths and E. D. Isaac, Proc. Roy. Soc. (London) A253, 1 (1959).

[8] L. F. Bates and D. J. Craik, J. Phys. Soc. Japan 17, Suppl. B1, 535 (1962).
[9] J. S. Sallo and J. M. Carr, J. Appl. Phys. 33, Suppl., 1316 (1962).
[10] K. J. Kronenberg, J. Appl. Phys. 33, Suppl., 1326 (1962).
[11] R. I. Hutchinson, P. A. Lavin and J. R. Moor, J. Sci. Instrum. 42, 885 (1965).
[12] H. Schwartze, Ann. d. Phys. 19, 322 (1957).
[13] G. V. Spivak et al., Izv. Akad. Nauk SSSR, ser. fiz. 21, 1177 (1957); M. Saad El-Din, A. M. Dubinina, G. V. Spivak and others, ibid. 24, 1567 (1970); Proceed. ICEM, Grenoble, v. 2, 1970, p. 597.
[14] L. V. Lazareva and G. V. Spivak, Izv. Akad. Nauk SSSR, ser. fiz. 25, 742 (1961).
[15] L. H. Germer, Phys. Rev. 62, 295 (1942).
[16] G. Scheidler, Arbeitstagung Festkorperphysik, in Dresden, Barth, Leipzig, 1955, p. 181.
[17] L. Marton, J. Appl. Phys. 19, 687 (1948).
[18] L. Marton, Phys. Rev. 73, 1475 (1948).
[19] L. Marton and S. H. Lachenbruch, J. Appl. Phys. 20, 1171 (1949).
[20] L. Marton, S. H. Lachenbruch, J. A. Simpson and A. Van Bronkhorst, J. Appl. Phys. 20, 1258 (1949).
[21] L. Marton, J. A. Simpson and S. H. Lachenbruch, J. Res. Nation. Bur. Std. 52, 97 (1954).
[22] L. T. Soboleva, Izv. Akad. Nauk SSSR, ser. fiz. 18, 511 (1954).
[23] L. Marton, Bull. Am. Phys. Soc. 24, 27 (1949).
[24] L. Marton, J. Sci. Ind. Res. (India) 16A, 429 (1957).
[25] N. N. Malov, Usp. Fiz. Nauk 41, 244 (1950).
[26] V. N. Gusev and B. A. Krasyuk, Tezisy VII Vsesoyuznoĭ konferentsii po élektronnoĭ mikroskopii, Kiev (1969), Sektsiya II, Tverdoe telo (Abstracts of Seventh All-union Conf. on Electron Microscopy, Kiev (1969), Sec. II, Solid State), M., 1969, p. 97; Fizika i khimiya obrabotki materialov (Physics and Chemistry of Material Finishing), No. 5, 40 (1969); Dokl. Akad. Nauk SSSR 188, 311 (1969) [Sov. Phys.-Dokl. 14, 881 (1970)].
[27] V. N. Gusev, B. A. Krasyuk, V. A. Lunev and V. M. Stratonov, Izv. Akad. Nauk SSSR, ser. fiz. 34, 1560 (1970).
[28] W. Rollwagen and Ch. Schwink, Optik 10, 525 (1953).
[29] Ch. Schwink, Optik 12, 481 (1955).
[30] H. Murrmann and Ch. Schwink, Zs. Angew. Phys. 10, 376 (1958); 13, 189, 192 (1961); Zs. Phys. 174, 536 (1963).
[31] H. Murrmann, Zs. Phys. 165, 305 (1961).
[32] Ch. Schwink, Zs. Phys. 161, 560 (1961); 173, 542 (1963).
[33] Ch. Schwink, H. Murrmann and H. Spreen, Zs. Angew. Phys. 14, 766 (1962).
[34] O. Grüter, H. J. Hafner, H. Murrmann and Ch. Schwink, Zs. angew. Phys. 18, 464 (1965).
[35] Ch. Schwink and O. Scharpf, Phys. Stat. Sol. 30, 637 (1968).
[36] O. Scharpf, Ch. Schwink and W. Feller, Zs. angew. Phys. 28, 158 (1969).
[37] J. M. Rodgers, J. Appl. Phys. 38, 1301 (1967).
[38] M. R. Lipschutz and J. M. Rodgers, J. Appl. Phys. 40, 1225 (1969).
[39] M. Blackman and E. Grünbaum, Proc. Roy. Soc. (London) A241, 508 (1957).
[40] M. Blackman, G. Haigh and N. D. Lisgarten, Nature 179, 1288 (1957).
[41] M. Blackman and E. Grünbaum, Proc. Roy. Soc. (London) A245, 408 (1958).
[42] A. E. Curzon, Ph. D. Thesis, University of London (1959).
[43] M. Blackman and N. D. Lisgarten, Phil. Mag. 3, 1069 (1958).
[44] M. Blackman and E. Grünbaum, Nature 180, 1189 (1957).
[45] M. Blackman, G. Haigh and N. D. Lisgarten, Proc. Roy. Soc. (London) A251, 117 (1959).
[46] G. Kaye, Proc. Phys. Soc. (London) 78, 869 (1961).
[47] G. Kaye, Proc. Phys. Soc. (London) 80, 238 (1962).
[48] M. Blackman and G. Kaye, J. Phys. Soc. Japan 17, 289 (1962).
[49] M. Blackman, G. Haigh and N. D. Lisgarten, Proc. Phys. Soc. (London) 81, 244 (1963).
[50] M. N. Rukosuev, A. I. Dryukin and G. I. Zyryanov, FMM 22, 548 (1966).
[51] M. Blackman, A. E. Curzon and A. T. Pawlowicz, Nature 200, 157 (1963).
[52] M. J. Goringe and U. Valdre, Proc. 3d Europ. Conf. Electron Microscopy, Prague, A, 305 (1964).
[53] G. Pozzi and U. Valdre, Proc. 4th Europ. Conf. Electron Microscopy, Rome, Italy 1, 355 (1968); G. Pozzi, Proc. ICEM, Grenoble, v. 1, 1970, p. 305.
[54] A. E. Curzon and N. D. Lisgarten, Adv. Electronics and Electron Phys. 24, 109 (1968).
[55] S. Yamaguchi, Japan. J. Appl. Phys. 28, 560 (1959).
[56] S. Yamaguchi and H. Sawamura, Zs. Metallkunde, 57, 590 (1966).
[57] S. Yamaguchi, Naturwiss. 48, 519 (1961); Zs. anorgan. und allgem. Chem. 314, 222 (1962); Phys. Rev. 126, 102 (1962); Brit. J. Appl. Phys. 14, 465 (1963); C. r. Acad. Sci. 264, B1703 (1967).
[58] S. Yamaguchi, Exp. Techn. Phys. 9, 304 (1961); J. Electrochem. Soc. 109, 346 (1962).
[59] S. Yamaguchi, Zs. Metallkunde 51, 340 (1960); J. Electrochem. Soc. 107, 714 (1960); Indian J. Phys. 33, 547 (1959); Indian J. Phys. 34, 535 (1960); Brit. J. Appl. Phys. 13, 248 (1962); Zs. Metallkunde 53, 259 (1962); Rev. Sci. Instrum. 33, 690 (1962); Naturwiss. 55, 489 (1968).
[60] S. Yamaguchi, Zs. Metallkunde 52, 248 (1961); J. Appl. Phys. 32, 961 (1961).
[61] S. Yamaguchi, Zs. Metallkunde 50, 721 (1959); Exp. Techn. Phys. 10, 244 (1962); J. Appl. Phys. 30, 1619 (1959); J. Chim. phys. et phys. chim. biol. 59, 101 (1962); Exp. Techn. Phys. 16, 437 (1968); Exp. Techn. Phys. 17, 164 (1969).
[62] S. Yamaguchi, Zs. Metallkunde 51, 461 (1960); Zs. Instrumentkunde 69, 224 (1961).
[63] S. Yamaguchi, Zs. Instrumentkunde 69, 244 (1961); J. Electrochem. Soc. 107, 55 (1960); Indian J. Phys. 33, 547 (1959); Zs. Instrumentkunde 68, 13 (1960).
[64] S. Yamaguchi, Brit. J. Appl. Phys. 18, 369 (1967); Exp. Techn. Phys. 15, 402 (1967); Phil. Mag. 17, 402 (1968); J. Iron and Steel. Instit. 206, 724 (1968); Rev. Sci. Instrum. 39, 1224 (1968); J. Phys. D (Brit. J. Appl. Phys.) ser. 2, 1, 1569 (1968); Messtechnik 77, 106 (1969).
[65] Sb. Élektronnaya mikroskopiya (Electron Micro-

scopy), ed. by A. A. Lebedev, Gostekhizdat, 1954.

[66] G. V. Spivak, N. G. Kanavina, I. S. Sbitnikova and I. N. Chernyshev, Dokl. Akad. Nauk SSSR 92, 541 (1953).

[67] G. V. Spivak, N. G. Kanavina, I. S. Sbitnikova and T. N. Dombrovskaya, Dokl. Akad. Nauk SSSR 105, 706 (1955).

[68] G. V. Spivak and T. N. Dombrovskaya, Dokl. Akad. Nauk SSSR 106, 39 (1956) [Sov. Phys.-Dokl. 1, 9 (1956)].

[69] I. S. Sbitnikova, G. V. Spivak and I. M. Saraeva, Izv. Akad. Nauk SSSR, sr. fiz. 23, 734 (1959).

[70] I. S. Sbitnikova, G. V. Spivak and I. M. Saraeva, in: Magnitnaya struktura ferromagnetikov (Magnetic Structure of Ferromagnets), ed. by L. V. Kirenskii, Novosibirsk, 1960, p. 41.

[71] G. V. Spivak, T. N. Dombrovskaya and N. N. Sedov, Dokl. Akad. Nauk SSSR 113, 78 (1957) [Sov. Phys.-Dokl. 2, 120 (1959)].

[72] G. V. Spivak and V. I. Lyubchenko, Izv. Akad. Nauk SSSR, ser. fiz. 23, 697 (1959).

[73] N. N. Sedov, G. V. Spivak and N. F. Isaeva, ibid. 25, 725 (1961).

[74] G. V. Spivak, R. D. Ivanov, O. P. Pavlyuchenko, N. N. Sedov and V. F. Shvets, ibid. 27, 1210 (1963).

[75] G. V. Spivak, N. N. Sedov, V. G. Dyukov and V. A. Khrustalev, ibid. 32, 1164 (1968).

[76] N. N. Sedov, G. V. Spivak and V. G. Dyukov, ibid. 32, 1134 (1968).

[77] N. N. Sedov, ibid. 32, 1175 (1968).

[78] N. N. Sedov, J. Microscopie 9, 1 (1970).

[79] N. N. Sedov, Izv. Akad. Nauk SSSR, ser. fiz. 33, 426 (1969).

[80] N. N. Sedov, Tezisy VII Vsesoyuznoĭ konferentsii po élektronnoĭ mikroskopii, Kiev (1969), Sektsiya 1, Élektronnaya optika i priborostroenie (Abstracts of Seventh All-union Conf. of Electron Microscopy, Kiev (1969), Sec. I, Electron Optics and Instrument Building), M., 1969, p. 32, 33; Izv. Akad. Nauk SSSR, ser. fiz. 34, 1529 (1970).

[81] G. V. Spivak, G. V. Saparin and M. V. Bykov, Usp. Fiz. Nauk 99, 635 (1969) [Sov. Phys.-Usp. 11, 756 (1970)].

[82] A. Speth, Rev. Sci. Instr. 40, 1636 (1969).

[83] V. N. Vertsner, R. I. Lagunov and Yu. V. Chentsov, Izv. Akad. Nauk SSSR, ser. fiz. 30, 778 (1966).

[84] J. R. Dorsey, Proc. 1st Nat. Conf. Electron Probe Microanalysis, Maryland, USA (1966).

[85] J. R. Banbury and W. C. Nixon, J. Sci. Instrum. 44, 889 (1967).

[86] J. R. Banbury and W. C. Nixon, Proc. 4th Europ. Conf. Electron Microscopy, Rome, Italy 1, 93 (1968); J. Phys. E, ser. 2, 2, 1055 (1969).

[87] W. C. Nixon, Proc. 4th Europ. Conf. Electron Microscopy, Rome, Italy, 1, 67 (1968); J. Phys. D, ser. 2, 2, 1367 (1969).

[88] D. C. Joy, J. P. Jakubovics, Phil. Mag. 17, 61 (1968).

[89] D. C. Joy and J. P. Jakubovics, Proc. 4th Europ. Conf. Electron Microscopy, Rome, Italy, 1, 85 (1968).

[90] G. V. Spivak, G. V. Saparin, N. N. Sedov and L. F. Komolova, Izv. Akad. Nauk SSSR, ser. fiz. 32, 962 (1968).

[91] G. V. Saparin, G. V. Spivak, N. N. Sedov and L. F. Comolova, Proc. 4th Europ. Conf. Electron Microscopy, Rome, Italy, 1, 87 (1968).

[92] N. N. Sedov, G. V. Spivak, G. V. Saparin and V. G. Galstyan, Radiotekhnika i élektronika 13, 2278 (1968).

[93] N. N. Sedov, V. G. Galstyan and L. F. Komolova, op. cit.[80], p. 36.

[94] G. Spivak, G. V. Saparin, G. T. Sbezhnev and N. F. Pesotskiĭ, Izv. Akad. Nauk SSSR, ser. fiz. 32, 967 (1968).

[95] R. F. M. Thornley and J. D. Hutchison, Appl. Phys. Lett. 13, 249 (1968).

[96] R. F. M. Thornley and J. D. Hutchison, Abstracts Intermag 69, Amsterdam, The Netherlands, 7.4 (1969).

[97] R. F. M. Thornley and J. D. Hutchison, Res. Develop. 20, 20 (1969); IEEE Trans. Magnet., MAG-5, 271 (1969).

[98] L. Mayer, J. Appl. Phys. 26, 1228 (1955).

[99] M. E. Barnett and W. C. Nixon, Proc. 3d Europ. Conf. Electron Microscopy, Prague, A, 37 (1964).

[100] L. Mayer, Electron Mirror Microscopy, in ''Encyclopedia of Microscopy'', Ed. by J. L. Clark, New York, vol. 3 (1961), p. 316.

[101] A. B. Bok, A Mirror Electron Microscope, Hoogland-Waltmann, Delft, 1968.

[102] G. V. Spivak, I. A. Pryamkova, D. V. Fetisov, A. N. Kabanov, L. V. Lazareva and A. I. Shilina, Izv. Akad. Nauk SSSR, ser. fiz. 25, 683 (1961).

[103] L. Mayer, R. Rickett and H. Stenemann, Proc. 5th Internat. Congr. Electron, Microscopy, Philadelphia 1, D-10 (1962).

[104] D. Wiskott, Optik 13, 379 (1956).

[105] W. Schwartze, Naturwiss. 52, 448 (1965).

[106] G. V. Spivak, I. N. Prilezhaeva and V. K. Azovtsev, Dokl. Akad. Nauk SSSR 105, 965 (1955).

[107] G. V. Spivak, I. A. Pryamkova and É. Igras, Izv. Akad. Nauk SSSR, ser. fiz. 23, 729 (1959).

[108] L. Mayer, J. Appl. Phys. 28, 975 (1957).

[109] G. V. Spivak and I. A. Pryamkova, in: Magnitnye struktury ferromagnetikov (Magnetic Structures of Ferromagnets), ed. by L. V. Kirenskiĭ, Novosibirsk, 1960, p. 185.

[110] L. Mayer, J. Appl. Phys. 30, 252S (1959).

[111] L. Mayer, J. Phys. Soc. Japan, 77, Suppl. B-1, 547 (1962).

[112] L. Mayer, J. Appl. Phys. 30, 1101 (1959).

[113] D. S. Lo, A. L. Olson and E. J. Torok, Rev. Sci. Instrum. 39, 259 (1968).

[114] G. V. Spivak, L. V. Kirenskiĭ, R. D. Ivanov and N. N. Sedov, Izv. Akad. Nauk SSSR, ser. fiz. 25, 1465 (1961).

[115] G. V. Spivak, R. D. Ivanov, O. P. Pavlyuchenko and N. N. Sedov, ibid. 27, 1139 (1963).

[116] V. I. Petrov, G. V. Spivak and A. E. Luk'yanov, Vestnik MGU, ser. 3, No. 6, 102 (1967).

[117] N. N. Sedov, G. V. Spivak, V. I. Petrov, A. E. Luk'yanov and E. I. Rau, Izv. Akad. Nauk SSSR, ser. fiz. 32, 1005 (1968).

[118] G. V. Spivak, O. P. Pavlyuchenko and A. E. Luk'yanov, Izv. Akad. Nauk SSSR, ser. fiz. 30, 813 (1966).

[119] L. Mayer, J. Appl. Phys. 29, 1003 (1958).

[120] L. Mayer, J. Appl. Phys. 29, 658 (1958).

[121] C. Guittard, R. Vassoille and E. Pernoux, Compt. Rend. 264, B924 (1967).

[122] A. E. Luk'yanov, G. V. Spivak, É. I. Rau and R. S. Gvozdover, op. cit.[26], p. 95.

[123] A. E. Luk'aynov, G. V. Spivak, É. I. Rau and R. S.

Gvozdover, Izv. Akad. Nauk SSSR, ser. fiz. **34**, 1539 (1970).
[124] G. V. Spivak and A. E. Luk'yanov, ibid. **30**, 803 (1966).
[125] A. E. Luk'yanov, G. V. Spivak, R. S. Gvozdover, V. G. Dyukov and N. N. Sedov, ibid. **32**, 1039 (1968).
[126] L. Mayer, Proc. 5th Internat. Congr. Electron Microscopy, Philadelphia 1, JJ-2 (1962).
[127] J. Kranz and H. Bialas, Optik 18, 178 (1961).
[128] N. N. Sedov, G. V. Spivak, V. I. Petrov and A. E. Luk'yanov, Radiotekhnika i élektronika **13**, 379 (1968).
[129] G. V. Spivak, O. P. Pavljutshenko, R. D. Ivanov, and G. P. Netischenskaja, Proc. 3rd Europ. Conf. Electron Microscopy, Prague, **A**, 293 (1964).
[130] R. D. Ivanov, Zh. Tekh. Fiz. 35, 145 (1965) [Sov. Phys.-Tech. Phys. 10, 110 (1965)].
[131] O. Bostanjoglo and G. Siegel, Cryogenics **7**, 157 (1967).
[132] A. E. Luk'yanov, G. V. Spivak, N. N. Sedov and V. I. Petrov, Izv. Akad. Nauk SSSR, ser. fiz. **32**, 987 (1968).
[133] G. V. Spivak, R. S. Gvozdover, A. E. Luk'yanov, N. N. Sedov, V. I. Petrov and A. I. Butylkin, ibid. **32**, 1211 (1968).
[134] A. E. Luk'yanov, N. N. Sedov, G. V. Spivak and R. S. Gvosdover, Proc. 4-th Europ. Conf. Electron Microscopy, Rome, Italy, 1, 105 (1968).
[135] V. I. Petrov and others, Vest. MGU, ser. 3, No. 4, 441 (1969); Proc. ICEM, Grenoble, v. 2, 1970, p. 25.
[136] V. N. Vertsner and Yu. V. Chentsov, PTÉ, No. 5, 200 (1963).
[137] J. R. Garrood and W. C. Nixon, Proc. 4th Europ. Conf. Electron Microscopy, Rome, Italy, 1, 95 (1968).
[138] S. Yamaguchi and H. Wada, J. Appl. Phys. 41, 1873 (1970).
[139] M. O. Coutts and E. R. Levin, Proc. ICEM, Grenoble, v. 1, 1970, p. 261.
[140] D. C. Joy et al., Phil. Mag. 20, 843 (1969).

Translated by J. G. Adashko